Particle Exchange in an Unstable Jet

M. SUSAN LOZIER* AND DAVID BERCOVICI**

Woods Hole Oceanographic Institution, Woods Hole, Massachusetts

(Manuscript received 10 October 1991, in final form 17 March 1992)

ABSTRACT

A one-dimensional model of baroclinic instability is used to reconcile two differing interpretations on why neutrally buoyant floats cross the Gulf Stream more readily at subthermocline depths. The study compares the location of the steering level, where the particle speed matches the speed of a propagating meander, to the location of the minimum in the meridional potential vorticity gradient. The former locale is the expected site of a maxima in particle exchange, based on kinematic arguments, while the latter is the expected site based on potential vorticity dynamics. Model results show that the two levels are not coincident; in general, the steering level is deeper in the water column than the minimum in the potential vorticity gradient. Additionally, it is the steering level where the largest cross-stream particle exchange is expected to occur.

1. Introduction

In the maintenance of an ocean gyre's balance of heat, salt, potential vorticity, and other active or passive tracers, the exchange across a gyre front must be considered. If the ocean gyre is defined by a mean bounding streamline, the advection of properties across the gyre front by the mean flow is precluded as an exchange mechanism. Viable alternatives for cross-gyre exchange are eddy advective fluxes and small-scale dissipative effects. For the case of a frontal boundary such as the Gulf Stream, the former mechanism is certainly more visual, if not more important than the latter for such a strongly inertial flow. The meandering path of the Gulf Stream moves anomalously cold water into warm regions, and vice versa, thus affecting cross-gyre heat exchange. Likewise, other properties are blended. Another manifestation of eddy advection is particle or mass exchange from one gyre to the next, whereby a particle, having escaped from the meandering stream, carries anomalous properties into the neighboring gyre. During the past decade a striking amount of particle exchange has been observed across the Gulf Stream with the use of SOFAR and RAFOS floats (Owens 1984; Bower and Rossby 1989). These float studies have shown that the extent of the observed particle exchange is depth dependent. In general, floats at shallow depths (upper thermocline) leave the stream less readily than those at deeper levels (lower thermocline), as is illustrated in Fig. 1 for a collection of 37 RAFOS floats. Each plotted trajectory represents a float's path from its launch position near Cape Hatteras until its first escape from the Gulf Stream. On average, the floats on the warmer surface were retained in the Stream for a considerably longer distance than those on the colder surface.

Likewise, in a study of cross-gyre exchange within the context of a quasigeostrophic eddy-resolving general circulation model, Lozier and Riser (1990) found that Lagrangian pathways cross a midlatitude jet, which acts as a frontal boundary between two wind-driven gyres. As with the observed particle exchange, the particle exchange within their three-layer model is also depth dependent; exchange increases with depth.

Two interpretations for this depth dependence in float behavior have been offered. A simple kinematic argument attributes the exchange across the Stream to the difference between a particle's speed (U) and the phase speed of the stream's meanders (c) (Owens 1984; Bower 1991). When $U \gg c$, the stream's meander is essentially a stationary wave during the time of a particle's transit downstream, thus allowing the particle to stay in the meandering stream. In such a case the particle's trajectory would deviate but slightly from an instantaneous streamline. Conversely, when $U \ll c$, the meander leaves the particle behind such that particles are no longer within the meandering stream. For this case, particle trajectories deviate significantly from instantaneous streamlines. Therefore, based on this kinematic argument alone, particle exchange is enhanced below a steering level (where $U = c$) and inhibited above for a monotonically decreasing velocity profile.

From their work with Lagrangian pathways, Lozier and Riser (1990) suggested that the conservation of potential vorticity was an important dynamic constraint that controlled the varying degree of exchange

* Present affiliation: School of the Environment and Department of Geology, Duke University

** Present affiliation: Department of Geology and Geophysics, University of Hawaii.

Corresponding author address: Dr. M. Susan Lozier, Department of Geology, Duke University, Durham, NC 27706.

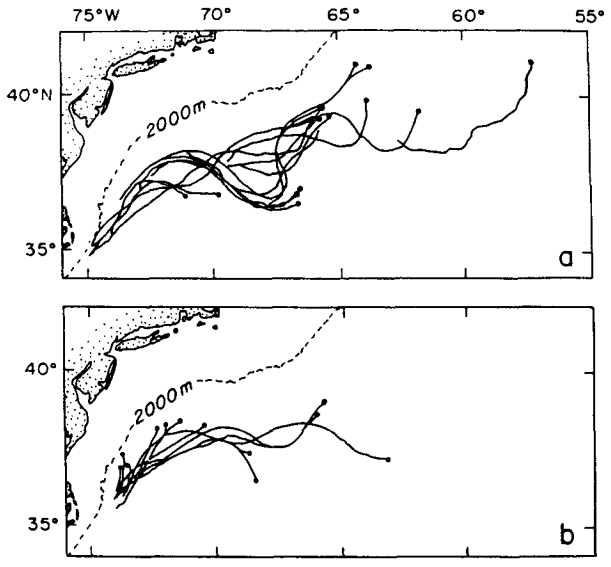

FIG. 1. Trajectories of RAFOS floats up to the point of first escape on temperature surfaces between (a) 11° and 16°C and (b) 7° and 11°C (from Bower and Rossby 1989).

with depth. They suggested that particle exchange was inhibited in the upper layer (of a three-layer model) due to the existence of a very strong potential vorticity gradient and that exchange was more prevalent in the lower layers where there was a much weaker gradient. Thus, they postulated that the varying degree of particle exchange with depth was strongly dependent upon the vertical structure of the meridional potential vorticity gradient such that the minimum in the gradient would be the expected site of the largest exchange.

This paper presents work that seeks to reconcile these two explanations for depth-dependent particle exchange. Thus, the primary question addressed is: Where is the location of the steering level relative to a minimum in the potential vorticity gradient? Second: What is the behavior of particles at each of these levels if they are not coincident? By addressing these questions we hope to further understand the depth variation of at least one component of cross-gyre communication.

2. Methods

To address the questions in this study, neither framework from which the two interpretations were made is appropriate. In order to locate a steering level based on a background potential vorticity gradient, U and c must be dynamically coupled; thus, a kinematic model would not suffice. Although an eddy-resolving general circulation model dynamically couples U and c, its inherent complexity, with a midlatitude jet characterized by a myriad of mixed instabilities, makes this medium also unsuitable. For this study a simple one-dimensional model of baroclinic instability has been chosen as the framework that contains the necessary dynamics in the simplest form. In using this model we are implicitly assuming that the propagating meanders that characterize a gyre front, such as the Gulf Stream, are the result of a baroclinically unstable zonal flow. Johns (1988) has shown that the gross characteristics of the Gulf Stream's meanders can be predicted from a simple, one-dimensional model of baroclinic instability where a cross-stream mean velocity profile was used.

The model used for this study consists of a steady, zonal background flow $U(z)$ such that

$$-\frac{\partial \Psi}{\partial y}(y, z) = U(z),$$

where Ψ is the horizontal streamfunction of the background flow and x, y, and z are the zonal, meridional, and vertical directions, respectively. A perturbation, ϕ, is imposed on the background flow such that the streamfunction of the perturbed state is given by

$$\psi(x, y, z, t) = \Psi(y, z) + \phi(x, z, t). \quad (1)$$

The flow is governed by the well-known quasigeostrophic potential vorticity equation,

$$\left(\frac{\partial}{\partial t} - \frac{\partial \psi}{\partial y}\frac{\partial}{\partial x} + \frac{\partial \psi}{\partial x}\frac{\partial}{\partial y}\right) \times \left(\nabla^2\psi + \beta y + \frac{\partial}{\partial z}\left(\frac{f_0^2}{N^2}\frac{\partial \psi}{\partial z}\right)\right) = 0, \quad (2)$$

where f_0 and β are the Coriolis parameter and its meridional gradient, respectively, and N^2 is the Brunt–Väisälä frequency.

Before proceeding further, Eq. (1) is expressed in nondimensional terms. With primes denoting nondimensional quantities the scale selections are

$$x = x'L$$
$$y = y'L$$
$$z = z'D$$
$$u = u'U_0$$
$$v = v'U_0$$
$$\psi = \psi'U_0L$$

and

$$t = t'L/U_0,$$

where L is the horizontal length scale of the problem, D is the vertical thickness of the water column ($0 \leq z \leq D$) and $U_0 = U(z' = 1)$. Substitution of these scalings into (1) yields (with the primes henceforth dropped from all variables)

$$\left(\frac{\partial}{\partial t} - \frac{\partial \psi}{\partial y}\frac{\partial}{\partial x} + \frac{\partial \psi}{\partial x}\frac{\partial}{\partial y}\right)\left(\nabla^2\psi + \beta_0 y + \frac{1}{S}\frac{\partial^2 \psi}{\partial z^2}\right) = 0, \quad (3)$$

where $\beta_0 = \beta L^2/U_0$ and $S = N^2D^2/f_0^2L^2$. The former is the beta Rossby number, and the latter is the Burger number, the ratio of the Rossby radius of deformation, $L_\rho = ND/f_0$, to the length scale of the flow [i.e., $S = (L_\rho/L)^2$].

Locally, the perturbation is considered to be a superposition of plane waves since the scale of the disturbance is assumed to be small compared to the horizontal scale of the gradients in the background flow. With this plane wave assumption, the perturbation streamfunction may be written as

$$\phi(x, z, t) = \Phi(z)e^{ik(x-ct)}. \quad (4)$$

Substitution of the total streamfunction (mean plus perturbation) into the potential vorticity equation leads to

$$(U(z) - c)\left[\frac{\partial^2\Phi}{\partial z^2} - Sk^2\Phi\right] + \frac{\partial Q}{\partial y}\Phi = 0, \quad (5)$$

where Q_y is the background meridional potential vorticity gradient and is given by

$$\frac{\partial Q}{\partial y} = \beta_0 S - \frac{\partial^2 U}{\partial z^2}.$$

(Note that subscripts will be used in the text to concisely denote differentiation.) This study concentrates on cases where $\beta_0 = 0$, since, for strongly baroclinic fronts such as the Gulf Stream, the meridional gradient of planetary vorticity is generally an order of magnitude smaller than the potential vorticity gradient created by the vertical shear (Johns 1988). For a given velocity profile, $U(z)$, Eq. (5) and its boundary conditions (given below) form an eigenvalue problem for c, which is the complex phase speed given by

$$c = c_r + ic_i.$$

The boundary conditions for Eq. (5) are determined by prescribing the vertical velocity at the surface ($z = 1$) and bottom ($z = 0$) boundaries. The vertical velocity in quasigeostrophic flows, which is derived from a combination of the density conservation equation and the hydrostatic approximation (Warren and Wunsch, 1981), is expressed as

$$w = -\frac{f_0}{N^2}\frac{D}{Dt}\frac{\partial\psi}{\partial z}. \quad (6)$$

Expressing (6) in nondimensional terms requires a scaling for w, which for quasigeostrophy is chosen to be

$$w = w'\frac{U_0 D}{L}\left(\frac{U_0}{f_0 L}\right).$$

The inclusion of the Rossby number in the scaling expresses the fact that quasigeostrophic flows are quasihorizontal. Using this scaling, and those presented earlier, the nondimensional expression for the vertical velocity, upon substitution of Eqs. (1) and (4), becomes

$$w = -\frac{1}{S}ike^{ik(x-ct)}\left[(U - c)\frac{\partial\Phi}{\partial z} + \frac{\partial U}{\partial z}\Phi\right]. \quad (7)$$

For the case of a flat-bottom and rigid-lid ocean, we assume $w = 0$; thus, we require

$$\frac{\partial\Phi}{\partial z} = \frac{-\frac{\partial U}{\partial z}\Phi}{U - c}$$

at $z = 0$ and $z = 1$.

Our choice of velocity profile is dictated by three desires. First and foremost, we want an unstable velocity profile. The velocity profile chosen must therefore satisfy one of the necessary conditions for baroclinic instability for a flat-bottom ocean (Green 1960), as given by

1) Q_y must change sign in the depth interval $1 > z > 0$, or
2) the sign of Q_y must be opposite to that of U_z at $z = 0$, or
3) the sign of Q_y must be opposite to that of U_z at $z = 1$.

Second, we desire to restrict the instability to be of the interior type rather than a boundary instability. Thus, we choose $U_z = 0$ at both boundaries, and we require the first condition above to be met. Finally, we prefer a velocity profile that has only one inflection point ($U_{zz} = 0$) in the interval of interest, so that the meridional gradient of potential vorticity (Q_y) vanishes at one depth only. To meet each of these requirements we have chosen to represent $U(z)$ with the functional form of a single half cosine wave in a stretched vertical coordinate:

$$U(z) = \frac{1}{2}(1 - \cos\pi z^n).$$

The dimensionless velocity U is in the range $0 \leq U \leq 1$, and the variable n is a free parameter controlling the depth location of the inflection point, which for this functional form will be in the upper water column. This choice of velocity profile also meets our requirement that $U_z = 0$ at both boundaries, thus simplifying the boundary conditions to $\Phi_z = 0$ at $z = 0, 1$.

The inflection point, z_{infl}, of each velocity profile (i.e., for a given n) satisfies the transcendental equation

$$(n - 1)\tan(\pi z^n) + n\pi z^n = 0,$$

which can easily be solved numerically for a chosen n. Shown in Fig. 2a are the velocity profiles for $n = 1$, 2, 3, 4, and 5, which yield inflection points at $z = 0.5$, 0.76, 0.85, 0.88, and 0.91. In order to investigate the full range of possible inflections points we also consider velocity profiles of the form

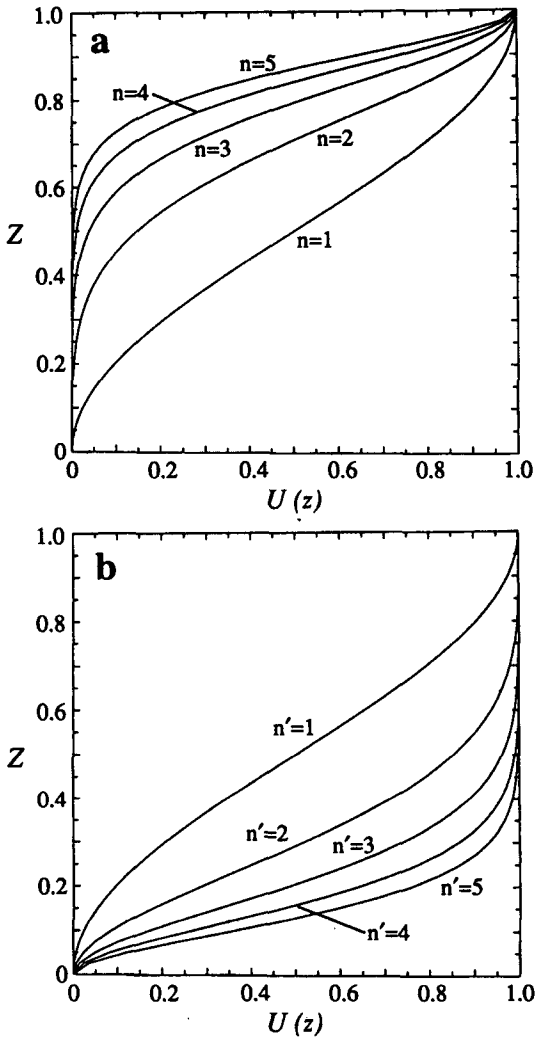

FIG. 2. Velocity as a function of depth for (a) inflection depths in the upper water column (n = 1 through 5) and (b) inflection depths in the lower water column (n' = 1 through 5).

$$U(z) = \frac{1}{2}[1 + (\cos\pi(1 - z)^{n'})],$$

where n' is the parameter controlling the location of the inflection point, which for these profiles will fall in the lower water column. Although these profiles are decidedly less realistic, they are included for completeness. For these profiles z_{infl} is found for a chosen n' from the numerical solution of

$$(n' - 1)\tan(\pi(1 - z)^{n'}) + n'\pi(1 - z)^{n'} = 0.$$

Figure 2b shows the velocity profiles for n' = 1, 2, 3, 4, and 5, which yield inflection points at z = 0.5, 0.24, 0.15, 0.12, and 0.09, respectively.

The solution approach is to solve Eq. (5) for $\Phi(z)$, c_r, and c_i for varying k values. Because we are interested in unstable perturbations, the range of k values that yields solutions such that $c_i > 0$ is sought. This two-point boundary value problem is well suited for solution by a shooting method (Press et al. 1989). Basically, the ordinary differential equation is numerically integrated from one boundary to the next using estimates for c_r and c_i and known boundary conditions at the first boundary. At the second boundary the mismatch between the computed boundary values and the known boundary conditions is used to reestimate c_r and c_i. This process is iterated until the discrepancy at the second boundary meets some predetermined tolerance.

Alternatively, this eigenvalue problem may be solved via an analytic Galerkin method. Briefly, the vertical coordinate of the problem is transformed into a stretched coordinate (i.e., $\zeta = z^n$), and then, $\Phi(\zeta)$ is expanded in a Fourier cosine series and substituted into the equation governing the instability, Eq. (5). A dispersion relation for c, as a function of k and S, results. This approach was used for the n = 1 and n = 2 cases; however, the secular determinant leading to the dispersion relation must be prohibitively higher order for any reasonable accuracy when $n > 2$, making the shooting method more expedient. The n = 1 and n = 2 cases were used to test the validity of the numerical scheme. Agreement between the two approaches, in a comparison of $c_i(k)$ and $c_r(k)$, was within 5%.

3. Results

In the following section the stability results from the numerical solution of Eq. (5) will be discussed. Because the baroclinic instability process favors length scales comparable to the Rossby radius of deformation (Pedlosky 1979), we take S = 1 for all cases. Because S appears only in the Sk^2 term in Eq. (5), a change in S would merely result in a shift of the wavenumber range. In the discussion to follow, the parameters n and n' are varied to yield a range of inflection points throughout the water column. Again, for the cases in this study (β_0 = 0) the inflection point locale corresponds to the zero in the meridional potential vorticity gradient. By systematically varying the Q_y = 0 location, its effect on the steering level locale is investigated.

a. Growth rates

For each velocity profile studied, a range of unstable wavenumbers results. Shown in Fig. 3 are the growth rates, kc_i, as a function of k for the n = 1, 2, 3, 4, and 5 velocity profiles. For all cases, the growth rates have a single maximum between the k = 0 limit and the point of marginal stability (where the curve intersects the abscissa axis at a nonzero k value). For the n = 1 case, the upper limit for unstable perturbations is at k = π. Thus, only perturbations with wavelengths longer than the length scale of the jet's vertical profile can extract potential energy from the system and grow. As n increases, the wavenumber range of unstable perturbations increases proportionally, allowing for smaller

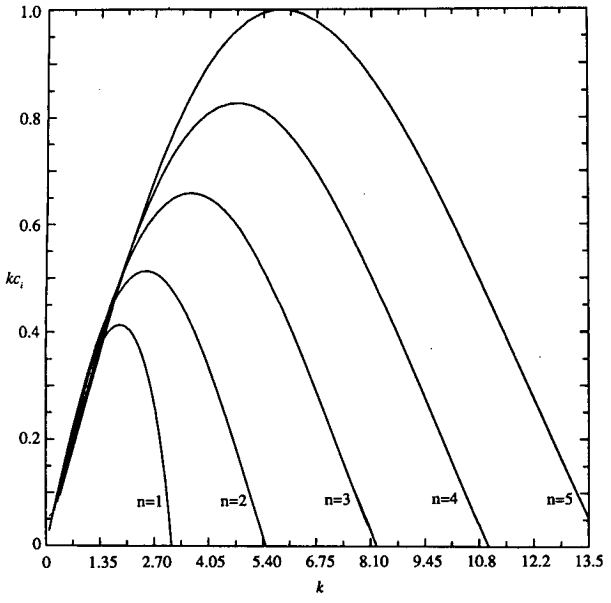

FIG. 3. Growth rate, kc_i, as a function of k for $n = 1, \cdots, 5$.

wavelengths to be unstable. Such a shift to smaller wavelengths may be explained by the fact that as n increases Q_y variations are confined to a narrower layer.

In general, for a given k the growth rates increase as n increases, except in the long wavelength limit where the growth rates are insensitive to the structure of the velocity profiles. As is evident from the velocity profiles in Fig. 2, an increase in n changes not only the depth of the inflection point but also the local values of U_z; as n increases there are larger local values of U_z in the water column. Using the thermal wind relation, such increases are proportional to increases in the meridional slope of the isopycnals. Therefore, results from Fig. 3 show that larger growth rates are associated with larger stores of available potential energy. For the small k limit (large wavelength), it is argued that the pertinent measure of vertical shear is that of the water column as a whole; namely, $[U(1) - U(0)]/D$. Since this measure is the same for all profiles, an insensitivity to background velocity structure results at smaller wavenumbers. Finally, the shift of the maximum growth rate to a higher wavenumber as n increases is noted.

As expected, the growth rate curves for the antisymmetric cases ($n' = 1, 2, 3, 4$, and 5), where the inflection points are located in the lower water column, are identical to the corresponding $n = 1, 2, 3, 4$, and 5 cases. Therefore, these curves are not reproduced. Differences between the cases will be noted later.

b. *Disturbance structure*

To facilitate a later discussion on steering levels, the vertical structure of the disturbance amplitude is briefly discussed here. Three representative cases, $n = 1, 3$, and 5 (Figs. 4a–c), are shown to illustrate how $|\Phi|$ varies with depth and with wavenumber. Because the magnitude of the disturbance is arbitrary, in all cases $|\Phi|$ has been set equal to unity at the upper boundary. For the $n = 1$ case, the perturbation streamfunction magnitude is symmetric about middepth for all wavenumbers. This symmetry is expected since the velocity and the meridional potential vorticity gradient are symmetric about middepth. For a nonsymmetric velocity case ($n \neq 1$) the disturbance structure is also nonsymmetric. The degree of asymmetry is wavenumber dependent; as k increases the disturbance becomes increasingly surface limited, as is illustrated for the $n = 3$ and 5 cases. Additionally, for a given wavenumber, as n increases the disturbance becomes increasingly surface limited, a reflection of the sharp gradients as the inflection point approaches the upper boundary. The $|\Phi|$ plots for the n' cases are the mirror images of the n cases. Thus, as k and n increase the disturbance becomes bottom intensified.

Though not shown here, the perturbation disturbance exhibits the characteristic increase of phase, $\theta(z)$, as z increases, a signature of baroclinic instability. As explained by Pedlosky (1979), lines of constant ϕ must be aligned westward and upward in regions where $U_z > 0$ (as is always the case for the profiles considered here) if the perturbations are to release any of the available potential energy of the mean flow.

c. *Steering levels*

Associated with each unstable wave is a phase speed, c_r, that determines the location of the steering level. Plotted in Fig. 5 is the depth of the steering level as a function of wavenumber for nine different velocity profiles. The n and n' values used here were chosen in order to produce evenly spaced inflection points at $z = 0.1$ ($n' = 4.52$), 0.2 ($n' = 2.33$), 0.3 ($n' = 1.60$), 0.4 ($n' = 1.23$), 0.5 ($n = n' = 1$), 0.6 ($n = 1.23$), 0.7 ($n = 1.60$), 0.8 ($n = 2.33$), and 0.9 ($n = 4.52$). This set of n values will be used for the remaining discussion. The different lengths for the curves are due to the differences in the unstable wavenumber range as n changes. Keeping in mind that the inflection depths are located at $z = 0.9$ through 0.1 for the uppermost to the lowermost curve, respectively, it is noted that only for the wavenumber of marginal stability (the nonzero k value where $c_i = 0$) does the steering level coincide with the inflection depth. A notable exception is the $n = n' = 1$ case where for all k the two levels coincide. For this symmetric case the phase speed is independent of the wavenumber and always equals the velocity at middepth. For the upper water column profiles, the inflection depth represents an upper limit on the steering levels, while for the lower water column profiles the inflection depth is a lower limit. The symmetry of the n and n' cases should also be noted.

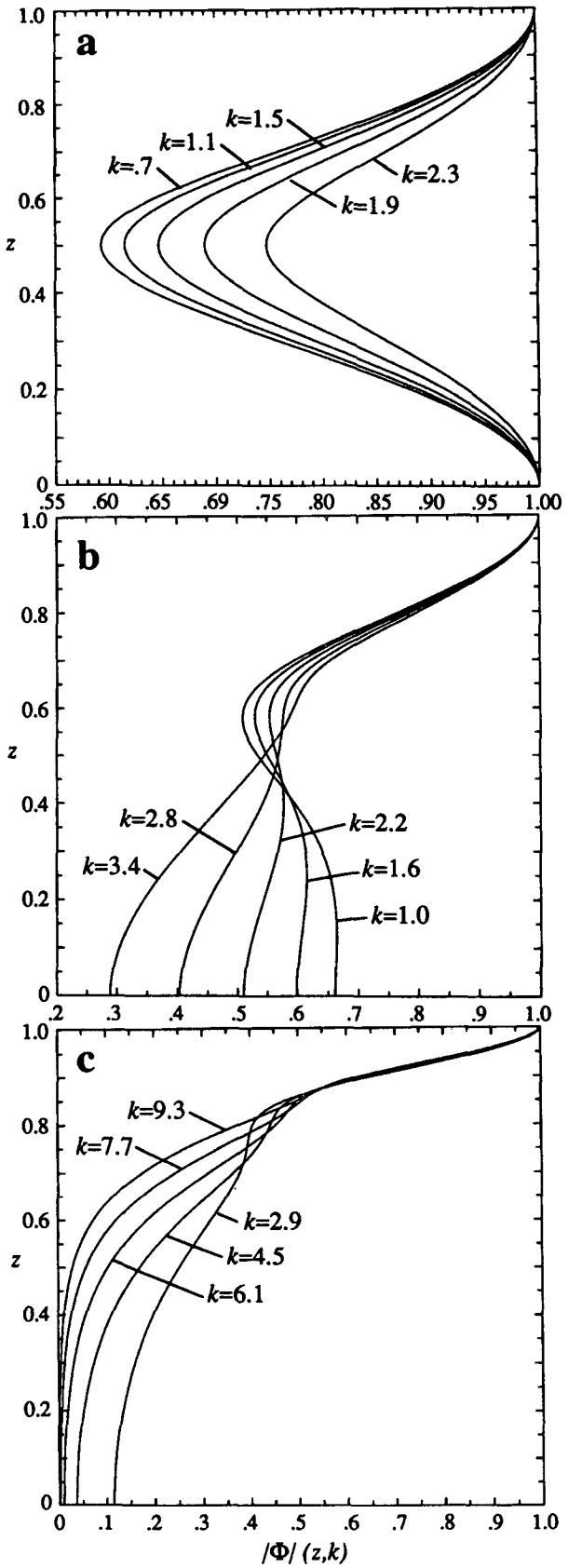

FIG. 4. $|\Phi|(z)$ for selected unstable wavenumbers for (a) $n = 1$, (b) $n = 3$, and (c) $n = 5$.

4. Discussion of results

a. Particle excursion and dispersion

Given that for unstable waves the steering level and inflection depth do not coincide, the question becomes which level, if either of these two, has the largest cross-stream excursion. To answer this, the equations governing a particle's motion are considered. At any time t a particle's displacement in the (x, y) plane is found from the integrations $\eta = \int (\partial\phi/\partial x)dt$ and $\xi = \int (-\partial\psi/\partial y)dt$, where η is the cross-stream displacement and ξ is the downstream displacement. In a coordinate system moving at speed $U(z)$ this integration yields

$$\xi = 0 \tag{8a}$$

and

$$\eta = \langle |\Phi| e^{kc_i t}\{(U - c_r)\cos[kt(U - c_r) + \Theta] - c_i \sin[kt(U - c_r) + \Theta]\}\rangle / |U - c|^2, \tag{8b}$$

where $\Theta = kx_0 + \theta(z)$, with x_0 the particle's initial location in the stream. Note that displacements are insensitive to y_0. As the particle moves with the stream, its cross-stream displacement is exponential with growth rate kc_i and periodic with a frequency of $k(U - c_r)$. For a given wavenumber, k, the quantity $k(U - c_r)$ is a depth-dependent frequency of the restoring oscillation. Although there is a tendency for the growth of the perturbation to cause exponential dispersion, a particle's cross-stream excursion is checked by the periodicity of the velocity field.

From Eq. (8b) it is evident that at the location where $U = c_r$ the particle's cross-stream motion is no longer periodic; the cross-stream displacement is solely exponential. Therefore, without any restoring oscillation the particle's cross-stream excursion is only to one side of the stream. Another way to view this behavior is to consider that if a particle is at the steering level then its location relative to a meander does not change. Given that the cross-stream velocity is defined by $\partial\phi/\partial x$, the cross-stream displacement will monotonically increase as the particle moves downstream. Therefore, without any restoring oscillation particles at this level will have the largest tendency to leave the stream. It is important to note here that this one-dimensional model does not allow for any distinction between the stream and its surroundings; the meridional extent of the flow field is infinite. Therefore, technically a particle does not leave the stream. The increasing displacement at the steering level is interpreted as a tendency for a particle to leave the stream if it had limits on its meridional extent. As particles move away from this level there is oscillatory motion, such that there is no net displace-

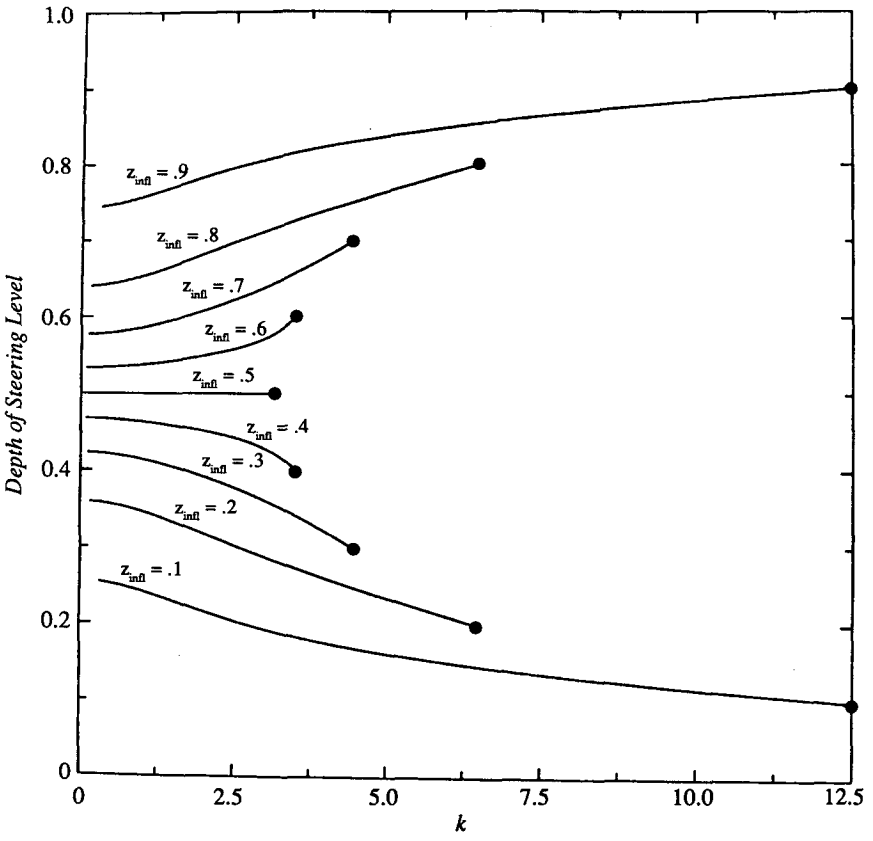

FIG. 5. Steering-level depth as a function of k for $n = 1, \cdots, 5$ and $n' = 1, \cdots, 5$.

ment of the particles over a temporal wavelength. It is important to note that according to Eq. (8b) it is the magnitude of $(U - c_r)$ that determines the strength of the restoring oscillation and not its sign. Thus, distinctions in particle behavior depend on whether the particles are at or away from the steering level, rather than above or below it, as interpreted in the kinematic models previously discussed.

Traditionally, a quantitative measure of particle behavior in a meandering stream has been the mean-square displacement, or particle dispersion. Using (8b), the particle dispersion is found to be

$$\overline{\eta^2} = \frac{\frac{1}{2}|\Phi|^2 e^{2kc_i t}}{|U - c|^2}. \tag{9}$$

Figure 6 shows this measure of particle dispersion (at $t = 0$) plotted as a function of depth for a range of unstable wavenumbers. For the symmetric case ($n = 1$) dispersion is largest at $z = 0.5$ for all wavenumbers, which is also the depth of the k-independent steering level. As z increases or decreases, dispersion decreases in a symmetric fashion, due to the equal magnitude change in $|U - c_r|$ and in $|\Phi|$.

In Fig. 6b a nonsymmetric case ($n = 3$), where the steering level is not at the same locale as the inflection depth, is presented. For all k, the largest dispersion occurs at the steering level, which is k dependent, and not at the inflection depth, which is k independent and located at $z = 0.7$. Thus, for the profiles chosen for this study, the largest particle dispersion occurs at the steering level. Such coincidence, however, need not always be the case. While the denominator of Eq. (9) will always be the smallest at the steering level, the depth-dependent amplitude could be such as to create maximum dispersion at a locale other than the steering level. For the profiles chosen for this study, the perturbation amplitudes are large in the vicinity of the steering levels. In the traditional Charney model of baroclinic instability, however, the largest dispersion occurs at the boundary where the amplitude is largest, yet the steering level falls in the interior. It must be kept in mind, however, that the Charney model is fundamentally different from this model since the conditions for instability are met by the boundary conditions and not by an interior change in the meridional potential vorticity gradient.

It is important to draw a distinction between maximum particle dispersion and maximum cross-stream particle excursions. In the latter case, particles uniformly deviate from their initial cross-stream location relative to the meander such that over a period they

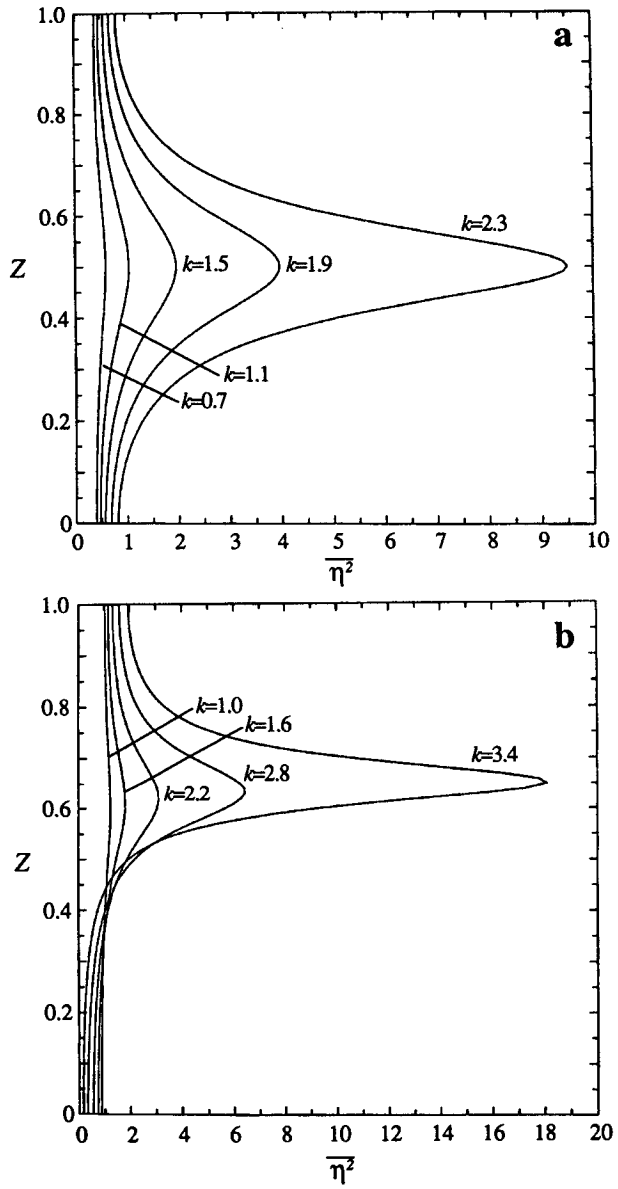

FIG. 6. Particle dispersion as a function of depth for selected unstable wavenumbers for (a) $n = 1$ and (b) $n = 3$.

have a net cross-stream displacement. In the former case, large mean-square displacements may occur because the meander itself has a large amplitude, yet a particle may stay close to its initial cross-stream location. Therefore, it is the steering level, with its nonoscillatory cross-stream particle excursions, that is of primary importance to cross-stream particle exchange.

b. *Potential vorticity conservation*

From the previous section it was shown that particles' cross-stream motion is uninhibited at the steering level. Given that in most cases ($n \neq 1$ and $c_i \neq 0$) a background cross-stream potential vorticity gradient exists at the depth of the steering level, the question becomes how particles cross this gradient. For this problem there are no sources or sinks of potential vorticity, so that there is conservation of the total potential vorticity along a particle's path,

$$\frac{Dq}{Dt} = 0 = \frac{DQ}{Dt} + \frac{Dq'}{Dt}, \tag{10}$$

where q' is used to denote the perturbation potential vorticity. For our problem Eq. (10) reduces to

$$\frac{\partial q'}{\partial t} + \frac{v\partial Q}{\partial y} + U\frac{\partial q'}{\partial x} = 0. \tag{11}$$

Multiplying by q' and spatially averaging over one wavelength in the x direction, Eq. (11) becomes

$$\frac{1}{2}\frac{\overline{\partial q'^2}}{\partial t} = -\overline{vq'}\frac{\partial Q}{\partial y}. \tag{12}$$

For a marginal or neutral wave, the left-hand side is zero. Thus, for any nonzero Q_y the mean flux of perturbation potential vorticity is zero; since q is conserved along a particle path, there is no mean flux of particles across a background Q gradient. The steering level for the marginal or neutral wave must therefore coincide with the level where $Q_y = 0$. For a growing wave, the left-hand side is nonzero and positive, thus allowing for downgradient fluxes of potential vorticity (i.e., $\overline{vq'}Q_y < 0$). Therefore, for a growing wave a steering level may occur at a nonzero Q_y level because unbounded particle motion is allowed for by growth in the particles' enstrophy.

c. *Location of steering level and wavenumber dependence*

For exponentially growing waves, the wave with the fastest growth rate, kc_i, will quickly dominate and presumably determine the instability characteristics of the flow field. The range of steering levels over all unstable wavenumbers (Fig. 5) is bracketed by the wavenumber at marginal stability [upper (lower) limit for the $n > 1$ ($n' > 1$) cases] and by the $k = 0$ limit [lower (upper) limit for the $n > 1$ ($n' > 1$) cases]. For all profiles the allowable range spans a maximum of approximately 15% of the water column. Thus, knowledge of these limits allows for an approximation of the steering level for the dominant wavenumber. As discussed earlier, the marginal stability limit has a steering level coincident with the level where $Q_y = 0$. As k decreases from this limit the steering level monotonically decreases (increases) for the $n > 1$ ($n' > 1$) cases until the $k = 0$ limit. For $k = 0$ the steering level occurs at the depth where $c_r = \int_0^1 U(z)dz$, as proven analytically in the Appendix. Thus, very long wavelength perturbations travel at the average speed of the water column.

For the symmetric case ($n = n' = 1$) the two limits are coincident; thus, the steering level range collapses to a single depth.

The wavenumber dependence for the steering level may be understood by a consideration of the necessary condition for instability. As shown earlier, for a growing wave, there exist nonzero perturbation potential vorticity fluxes throughout the water column. Because there are no external sources or sinks of potential vorticity the perturbation potential vorticity results from a redistribution of the background potential vorticity. The perturbation fluxes accomplish this redistribution in a baroclinic ocean by flattening the isopycnal surfaces, whose slope create the mean potential vorticity gradient. Because this is a conservative process this redistribution is constrained by

$$\int_0^1 \overline{vq'}\,dz = 0. \tag{13}$$

Thus, given the reversal of Q_y in the water column, the negative downgradient fluxes above the inflection depth must cancel the positive downgradient fluxes below. Alternatively, as the layers that thinned to the north thicken, the layers below thin to the north. Cancellation of these fluxes is dependent upon their relative magnitude with depth. To explicitly show how the flux depends upon the solution variables this constraint may be rewritten as

$$\int_0^1 \frac{kc_i|\Phi|^2}{|U-c|^2}\frac{\partial Q}{\partial y}e^{2kc_i t}\,dz = 0, \tag{14}$$

with the derivation given in Pedlosky (1979). From Eq. (14) it is evident that perturbation fluxes are large where Q_y and $|\Phi|$ are large and as the steering level is approached. For a given Q_y profile, as k changes, the depth structure of $|\Phi|$ changes, as noted earlier. For short waves $|\Phi|$ is intensified near the boundaries, while for long waves $|\Phi|$ is of considerable magnitude over the entire water column. Since $|\Phi|$ changes with depth, the depth-integrated flux remains zero through an adjustment in the denominator. Such an adjustment brings about changes in c_r (and also c_i), thus affecting a relocation of the steering level. Of course, it could also be argued that $|\Phi|(z)$ changes must occur to compensate for the wavenumber dependence of c_r and c_i; ultimately the three solution variables (Φ, c_r, and c_i) are interdependent as prescribed by the eigenvalue problem. The argument offered here attempts to explain steering level changes in response to k and $|\Phi|$ changes. In sum, because perturbations of differing wavelengths influence differing amounts of the water column, in order for the flattening of the isopycnals to be a conservative process (height is neither created nor destroyed), the perturbation phase speed must be wavelength dependent.

d. Numerical model results and observations

As stated in the Introduction, this study was motivated by some numerical model results and observations of particle exchange. A brief reconsideration of these aspects is warranted following the results of the prior sections.

A well-known and much studied feature of the family of quasigeostrophic eddy-resolving general circulation models (EGCM) is the pool of homogenized potential vorticity (no gradients in the background field) that occurs on an interior layer where there is no direct forcing or bottom friction. An examination of particle trajectories within this region of a three-layer EGCM [described in detail in Lozier and Riser (1990)] reveals that there is limited particle exchange across a midlatitude jet separating two wind-driven gyres. From an analysis of meander phase speeds it appears as though the homogenized region (in layer 2) lies above a steering level. For this three-layer model the vertical resolution is insufficient to resolve a steering depth, but it clearly lies below the $Q_y = 0$ level, in agreement with the results presented in this paper. To isolate a steering depth and to determine its proximity to a homogenized region, a model is needed that can sufficiently resolve the upper and lower limits of the steering levels. For background velocity profiles similar to those presented here, which place the two limits in close proximity, the needed resolution would be approximately 20 or 30 levels.

As previously mentioned, using observed velocity, stratification, and potential vorticity data, Johns (1988) determined the stability characteristics of the Gulf Stream near 74°W. A comparison of a steering level depth with the depth of a zero crossing in the Q_y profile is complicated by the fact that from this analysis there are three unstable modes and three zero crossings for Q_y. All three steering levels, however, fall in a region of negative Q_y values, below the first (and major) zero crossing. The steering level associated with the lowest-frequency mode (28 days, 380 km) is located at approximately 1300 m, which is below the depth spanned by all three zero crossings (700 m–1100 m). The fact that the steering levels do not coincide with the zero crossings and are, in general, below the zero crossings indicates that the results presented here are generally consistent with observations. Relating this predicted steering level back to RAFOS float behavior requires an assumption that the dominant instabilities remain basically unchanged from the time of the CTD and Pegasus observations used for Johns' work (1981–82) to the period January 1984–October 1985 when the RAFOS floats were seeded. Unfortunately, data is not available during the floats' transit to determine the temporally relevant steering level. However, if such an assumption is valid, then the RAFOS floats shown in both Figs. 1a and 1b are above the steering level determined by Johns. The floats on the warmer surface

clearly are in an area where $U > c$, but many of the deeper floats also exhibit meandering patterns, indicating a difference between U and c. Variability in these patterns can be attributed to variability in both U and c. For the deeper floats, which are on average at a depth of 1000 m, such variability could temporarily place them at a steering depth. Such a scenario could explain those few floats that leave the stream right after launch (Fig. 1b).

Finally, it is noted that comparisons with observations and numerical models must be viewed with caution given the simplifications of the baroclinic instability model presented in this paper. The main obstacle for comparisons is the lack of cross-stream structure for the profiles considered here. The overall result that the steering level does not coincide with a homogenized q region, however, is consistent with observations and modeling results.

5. Conclusions

Based on the one-dimensional baroclinic instability model used in this study, the steering level, in general, is not coincident with the level where the meridional potential vorticity gradient has its minimum. For velocity profiles with inflection depths in the upper water column, the depth of the zero in the meridional potential vorticity gradient is an upper limit for the steering level and the depth where the velocity equals the depth-averaged velocity is the lower limit. The steering level for the dominant unstable wave is bracketed by these two limits. For the profiles studied here these two limits are in close proximity; however, the amount of the water column spanned is entirely dependent upon the vertical structure of the velocity and potential vorticity fields. Furthermore, the basic profiles may be such as to switch the upper limit to a lower limit, and vice versa, as was demonstrated for the n' cases studied here. Regardless of the background profiles, the general result holds that these two levels bracket the allowable steering level range for unstable wavenumbers, with the provision that there is but one zero crossing. The location of the steering level, within this range, for a given wavenumber is heavily influenced by the dynamic constraint that the depth-integrated perturbation potential vorticity flux must be zero.

Due to nonoscillatory particle motion at a steering level, cross-stream exchange can be expected to be largest at a steering level and not at a level where the cross-stream potential vorticity gradient is weakest. Ease of exchange is characterized as enhanced at the steering level and inhibited above or below this level. Prior descriptions of particle exchange made divisions based on whether particles were above or below the steering level, rather than at or away from the steering level.

The major result of this work, that maximum particle exchange occurs where there is a background potential vorticity gradient, implies that such cross-stream exchange is an important contributor to eddy advective fluxes. A secondary implication of these results is that areas of homogenized potential vorticity do not have unbounded particle exchange, which would lead to strong mixing. This result supports the work of Rhines and Young (1982), where it is argued that weak mixing is required for homogenization.

An obvious and important extension of this work is to add a second dimension to the model, such that the zonal flow also varies meridionally. Instead of having a steering level, a steering surface would result. It is anticipated that such added dimensionality would deter particle escape from the stream, namely, because particle paths would not lie on a steering surface, or equivalently, isotachs. In other words, for a jet with cross-stream structure, cross-stream excursions would result in downstream velocity changes for a particle. If that particle were initially at a steering location, such a velocity change would end the particle's phase locking with the meander and a restoring oscillation would ensue. Clearly, with the added dimensionality, the notion of exchange being largest at a steering level is too simplistic. Thus, adding cross-stream structure would refine the ideas presented in this paper. Additionally, having a second dimension would aid the analyses since particle separation from the meandering stream would have a sharper definition, and of course, added dimensionality would move us a step closer to understanding the particulars of the Gulf Stream pathways. Finally, a second extension of this work is for the generalization of the velocity profiles.

Acknowledgments. The authors wish to gratefully acknowledge J. Pedlosky's role in the initiation and progress of this work. Thanks are also due to L. Pratt for many insightful discussions and for providing the calculation in the Appendix, to W. B. Owens for his support, and to M. A. Lucas for her help in the preparation of this manuscript. This work was conducted while both authors held postdoctoral fellowships at the Woods Hole Oceanographic Institution. Support from the Office of Naval Research, Grant N00014-86-K-0751 for M. S. Lozier and from the W. M. Keck Geodynamics Program for D. Bercovici is also acknowledged.

APPENDIX

Determination of Phase Speed at the Long-Wave Limit

For a basic flow, $U = U(z)$, with $U_z = 0$ at $z = 0, 1$, the linear stability problem reduces to

$$(U - c)(\Phi_{zz} - k^2\Phi) - \Phi U_{zz} = 0, \qquad (A.1)$$

with

$$\Phi_z = 0 \quad \text{at} \quad z = 0, 1 \qquad (A.2)$$

for $\beta_0 = 0$ and $S = 1$.

Using

$$(U-c)\Phi_{zz} - \Phi(U-c)_{zz} = [(U-c)^2(\Phi/(U-c))_z]_z,$$

Eq. (A.1) can be rewritten as

$$[(U-c)^2(\Phi/(U-c))_z]_z = k^2\Phi(U-c). \quad \text{(A.3)}$$

Substituting a long-wave expansion for Φ,

$$\Phi = \Phi^{(0)} + k^2\Phi^{(1)} + \cdots,$$

into Eq. (A.3) yields

$$[(U-c)^2(\Phi^{(0)}/(U-c))_z]_z = 0 \quad \text{(A.4)}$$

for the zeroth-order equation and

$$[(U-c)^2(\Phi^{(n)}/(U-c))_z]_z = (U-c)\Phi^{(n-1)} \quad \text{(A.5)}$$

for the nth-order equation, with $n = 1, 2, 3, \cdots$. The boundary conditions are

$$\Phi_z^{(n)} = 0 \quad \text{at} \quad z = 0, 1$$

for $n = 0, 1, 2, \cdots$.

Integrating Eq. (A.4) yields

$$(U-c)^2(\Phi^{(0)}/(U-c))_z = c_1.$$

Since the boundary condition at $z = 0$ yields

$$(\Phi^{(0)}/(U-c))_z = 0,$$

then $c_1 = 0$; thus,

$$\Phi^{(0)} = c_2(U-c).$$

Substituting this solution into the first-order equation $[O(k^2)]$ yields

$$[(U-c)^2(\Phi^{(1)}/(U-c))_z]_z = c_2(U-c)^2,$$

which, upon integration, yields

$$(U-c)^2(\Phi^{(1)}/(U-c))_z = c_2\int_0^z (U-c)^2 dz.$$

Applying the boundary condition at $z = 1$ causes the left-hand side to vanish; thus,

$$\int_0^1 (U-c)^2 dz = 0.$$

Separating this integral into real and imaginary parts yields the two conditions:

$$\int_0^1 [(U(z)-c_r)^2 - c_i^2]dz = 0$$

and

$$\int_0^1 (U(z)-c_r)dz = 0.$$

Thus, the real phase speed for the long-wave limit is given by

$$c_r = \int_0^1 U(z)dz,$$

and the imaginary phase speed is given by

$$c_i^2 = \int_0^1 U^2(z)dz - c_r^2.$$

REFERENCES

Bower, A. S., 1991: A simple kinematic mechanism for mixing fluid parcels across a meandering jet. *J. Phys. Oceanogr.*, **21**, 173–180.

——, and T. Rossby, 1989: Evidence of cross-frontal exchange processes in the Gulf Stream based on isopycnal RAFOS float data. *J. Phys. Oceanogr.*, **19**, 1177–1190.

Green, J. S. A., 1960: A problem in baroclinic stability. *Quart. J. Roy. Meteor. Soc.*, **86**, 237–251.

Johns, W. E., 1988: One-dimensional baroclinically unstable waves on the Gulf Stream potential vorticity gradient near Cape Hatteras. *Dyn. Atmos. Oceans*, **11**, 323–350.

Lozier, M. S., and S. C. Riser, 1990: Potential vorticity sources and sinks in a quasigeostrophic ocean: beyond western boundary currents. *J. Phys. Oceanogr.*, **20**, 1608–1627.

Owens, W. B., 1984: A synoptic and statistical description of the Gulf Stream and subtropical gyre using SOFAR floats. *J. Phys. Oceanogr.*, **14**, 104–113.

Pedlosky, J., 1979: *Geophysical Fluid Dynamics.* Springer-Verlag, 624 pp.

Press, W. H., B. P. Flannery, S. A. Teukolsky, and W. T. Vetterling, 1989: *Numerical Recipes. The Art of Scientific Computing (FORTRAN Version).* Cambridge University Press, 702 pp.

Rhines, P. B., and W. R. Young, 1982: A theory of wind-driven circulation: I. Mid-ocean gyres. *J. Mar. Res.*, **40**(Suppl), 559–596.

Warren, B. A., and C. Wunsch, 1981: *Evolution of Physical Oceanography: Scientific Surveys in Honor of Henry Stommel,* The MIT Press, 623 + xxxiii pp.